

Supporting Information For

Regulating near-infrared region to visible-light emission by adjusting cuprophilic interactions for blue light-excited phosphors

Guang-Ning Liu,^{*,a} Rang-Dong Xu,^a Jin-Shuang Guo,^{b,c} Jin-Ling Miao,^a Ming-Jian Zhang,^d and Cuncheng Li^a

^a*School of Chemistry and Chemical Engineering, University of Jinan, Jinan, Shandong 250022, P. R. China. E-mail: chm_liugn@ujn.edu.cn*

^b*Shandong Center for Food and Drug Evaluation & Certification, Jinan, Shandong 250014, P. R. China.*

^c*State Key Laboratory of Structural Chemistry, Fujian Institute of Research on the Structure of Matter, Chinese Academy of Sciences, Fuzhou, Fujian 350002, P. R. China*

^d*School of Advanced Materials, Peking University, Shenzhen Graduate School, Shenzhen 518055, P. R. China*

Contents

S1 Materials and characterization	3
S2 Computational details	3
S3 Single-crystal structure determination	4
Table S1	4
Table S2	5
Fig. S1	6
Fig. S2	7
IR analysis.....	7
Fig. S3	7
Fig. S4	8
Fig. S5	8
Fig. S6	9
Fig. S7	9
Fig. S8	9
Table S3	10
Table S4	10
Table S5	10
Fig. S9	10
Fig. S10	11
Fig. S11	11
Fig. S12	12
Table S6	12
Fig. S13	13
Fig. S14	14
Fig. S15	14
Fig. S16	15
Table S7	15
Fig. S17	15
Table S8	16
Table S9	16
Reference.....	24

S1 Materials and characterization

All reagents were purchased commercially and used without further purification. Cuprous iodide and 4-mercaptopyridine were provided by Macklin. Hydroiodic acid (45%) was purchased from Shanghai Kefeng Chemical Regent Co., Ltd. Ethanol and acetonitrile were purchased from Sinopharm Chemical Regent Co. Elemental analyses of C, H, and N were performed on an Elementar Vario EL III microanalyzer. Powder X-ray diffraction (PXRD) patterns were recorded on Bruker D8 Focus diffractometer using Cu $K\alpha$ radiation. A Mettler Toledo TGA/DSC1 thermogravimetric analyzer was used to obtain thermogravimetric analyses (TGA) curves in N_2 with a flow rate of $20 \text{ mL}\cdot\text{min}^{-1}$ and a ramp rate of $10 \text{ }^\circ\text{C}\cdot\text{min}^{-1}$ in the temperature range $40\text{--}800 \text{ }^\circ\text{C}$. An empty Al_2O_3 crucible was used as the reference. The FT-IR spectra were obtained on a Perkin-Elmer spectrophotometer using KBr disk in the range $4000\text{--}450 \text{ cm}^{-1}$. Optical diffuse reflectance spectra were measured at room temperature with a Shimadzu UV-3101 PC UV-vis spectrophotometer. The instrument was equipped with an integrating sphere and controlled with a personal computer. The samples were ground into fine powder and pressed onto a thin glass slide holder. A $BaSO_4$ plate was used as a standard (100% reflectance). The absorption spectra were calculated from reflectance spectrum using the Kubelka-Munk function:¹ $\alpha/S = (1-R)^2/2R$ where α is the absorption coefficient, S is the scattering coefficient, and R is the reflectance. The solid-state luminescence excitation and emission spectra were recorded on an Edinburgh FLS920 fluorescence spectrophotometer at room temperature. The integrated emission intensity was fitted using equation (1), in which I_0 is the intensity at 0 K, E_b the binding energy, and k_B the Boltzmann constant.² The absolute emission quantum yields were measured at room temperature using an integrating sphere on the Edinburgh FLS 920 spectrometer.

$$I(T) = \frac{I_0}{1 + Ae^{-E_b/k_B T}} \quad (1)$$

S2 Computational details

The X-ray crystallographic data were used to calculate its electronic structure. The calculations of density of states (DOS) were carried out using density functional theory (DFT)

with one of the three nonlocal gradient-corrected exchange-correlation functionals (GGA-PBE) and performed with the CASTEP code,³⁻⁴ which uses a plane wave basis set for the valence electrons and norm-conserving pseudopotential for the core electrons.⁵ Pseudo-atomic calculations were performed for Cu 3d¹⁰4s¹, S 3s²3p⁴, C 2s²2p², N 2s²2p³ and H 1s¹. The parameters used in the calculations and convergence criteria were set by the default values of the CASTEP code.³⁻⁴ The energies of the frontier molecular orbitals were calculated at the B3LYP/6-31G(d, p) level using the Gaussian 09 package.⁶

S3 Single-crystal structure determination

The intensity data sets were collected on a Agilent Xcalibur, Eos, Gemini CCD diffractometer equipped with a graphite-monochromated Mo K α radiation ($\lambda = 0.71073 \text{ \AA}$) at 293 K. The data sets were reduced by the CrysAlisPro⁷ program. An empirical absorption correction using spherical harmonics was implemented in SCALE3 ABSPACK scaling algorithm. The structures were solved by direct methods using the Siemens SHELXL package of crystallographic software.⁸ Difference Fourier maps were created on the basis of these atomic positions to yield the other non-hydrogen atoms. The structures were refined using a full-matrix least-squares refinement on F². All non-hydrogen atoms were refined anisotropically. The hydrogen atoms were located at geometrically calculated positions and refined as riding on their parent atoms with fixed isotropic displacement parameters [$U_{\text{iso}}(\text{H}) = 1.2U_{\text{eq}}(\text{C, N})$]. The Hirshfeld surfaces and the corresponding finger print plots were generated using Crystal Explorer17 software.⁹ Crystallographic data and structural refinements for the title compounds are summarized in Table 1. Important bond lengths and angles are listed in Table S1.

Table S1 Theoretical and experimental element content.

		C/ %	H/ %	N/ %
UJN-Cu3	Calculated	36.59	1.75	6.10
	Experimental	35.92	1.74	6.09
UJN-Cu4	Calculated	23.77	1.20	5.55
	Experimental	25.51	1.25	6.00

UJN-Cu5	Calculated	29.82	1.25	5.80
	Experimental	29.73	1.16	5.73

Table S2 Crystallographic data for UJN-Cu3, UJN-Cu4, and UJN-Cu5.

Compound	UJN-Cu3	UJN-Cu4	UJN-Cu5
Formula	C ₄₂ H ₂₄ N ₆ S ₁₂ Cu ₆	C ₃₀ H ₁₈ Br ₆ N ₆ S ₆ Cu ₆	C ₃₆ H ₁₈ F ₁₈ N ₆ S ₆ Cu ₆
<i>M_r</i> (g mol ⁻¹)	1378.63	1515.56	1450.16
Crystal system	Triclinic	Monoclinic	Monoclinic
Space group	P-1	<i>C2/c</i>	<i>C2/c</i>
ρ_{calcd} [g cm ⁻³]	1.915	2.370	2.072
<i>a</i> [Å]	7.6720(3)	23.5877(16)	26.2001(9)
<i>b</i> [Å]	13.3497(7)	9.5358(4)	9.5655(3)
<i>c</i> [Å]	13.8296(6)	18.9218(8)	18.8973(5)
α [°]	113.835(5)	90	90
β [°]	101.344(4)	93.488(5)	101.009(3)
γ [°]	102.954(4)	90	90
<i>V</i> [Å ³]	1195.27(11)	4248.1(4)	4648.8(3)
<i>Z</i>	1	4	4
<i>F</i> (000)	684	2880	2832
θ range [°]	3.247–25.50	3.362–25.50	3.168–25.50
Measured reflections	13677	12297	13455
Independent reflections (<i>R</i> _{int})	4448 (<i>R</i> _{int} = 0.0313)	3949 (<i>R</i> _{int} = 0.0629)	4319 (<i>R</i> _{int} = 0.0279)
Data/params/restraints	3494/298/0	2346/254/18	3468/325/36
<i>R</i> ₁ ^a , <i>wR</i> ₂ ^b [<i>I</i> > 2 <i>s</i> (<i>I</i>)]	0.0370, 0.0837	0.0601, 0.1127	0.0600, 0.1655
Goodness of fit	1.026	1.041	1.041
$\Delta\rho_{\text{max}}$ and $\Delta\rho_{\text{min}}$ [e Å ⁻³]	1.396, -0.594	0.873, -0.685	1.830, -0.984

$$^a R_1 = \sum ||F_o| - |F_c|| / \sum |F_o|, \quad ^b wR_2 = \{ \sum w[(F_o)^2 - (F_c)^2]^2 / \sum w[(F_o)^2]^2 \}^{1/2}$$

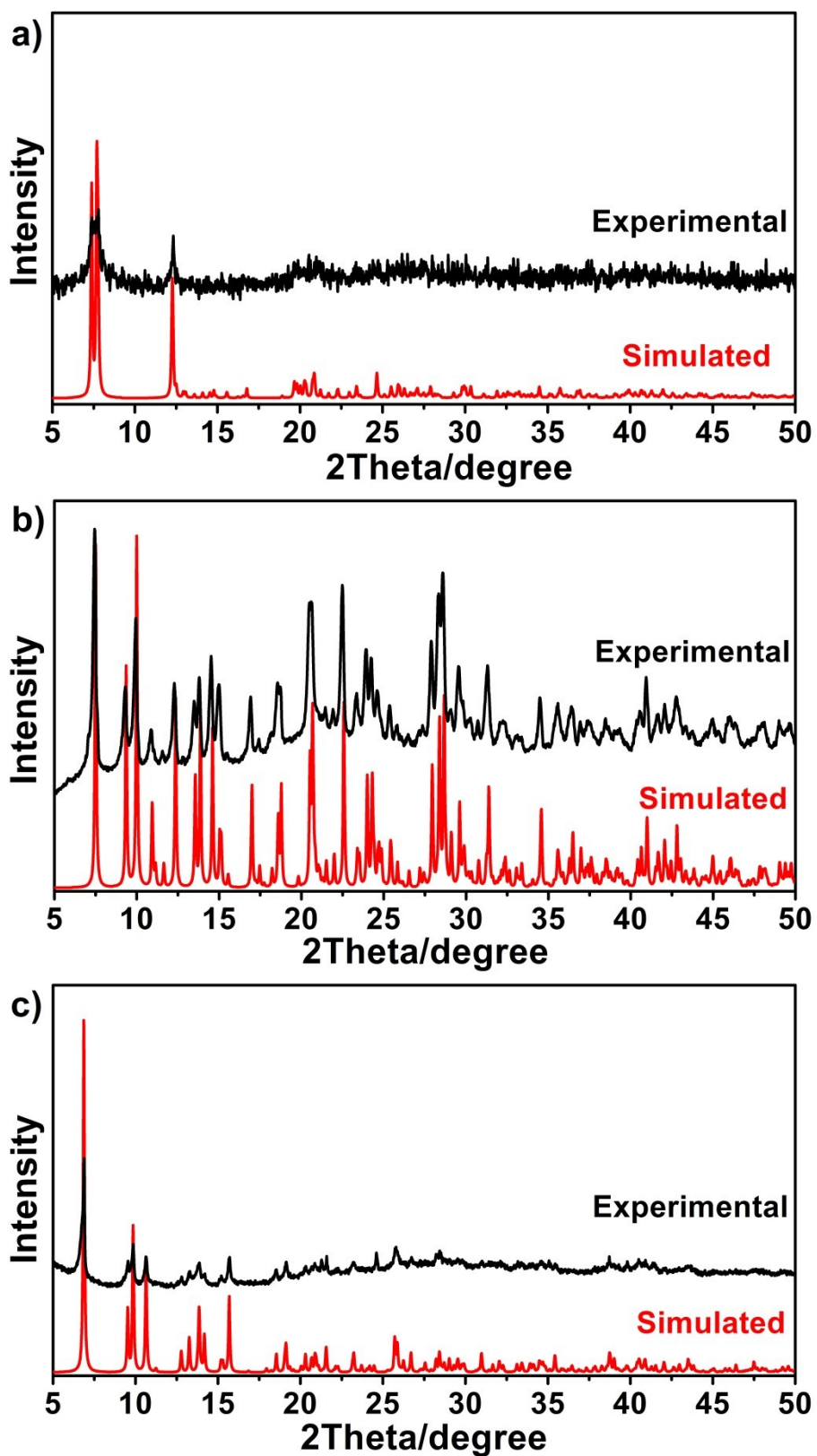


Fig. S1 The PXR D patterns for UJN-Cu3 (a), UJN-Cu4 (b), and UJN-Cu5 (c).

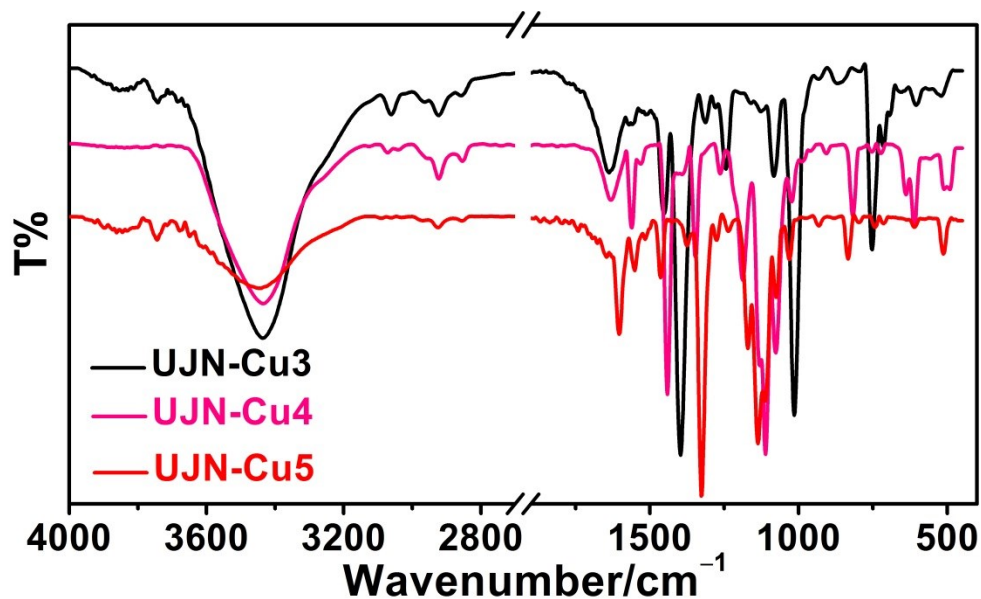


Fig. S2 IR spectra of UJN-Cu3, UJN-Cu4, and UJN-Cu5.

IR analysis: The relatively weak bands in the region of 3100–3020 cm^{-1} ascribed to the C–H vibrations of the aromatic ring hydrogen atoms, $\nu(\text{C–H})$. The bands of ring vibrations of the conjugated ligand ($\nu(\text{C=C})$ and $\nu(\text{C=N})$) are found at 1650–1400 cm^{-1} , indicating the presence of cmp cation. The strong band at $\sim 3433 \text{ cm}^{-1}$ is due to the stretching of trace water since the measurements were conducted in air. In brief, the above results are all in agreement with the single crystal X-ray diffraction studies.

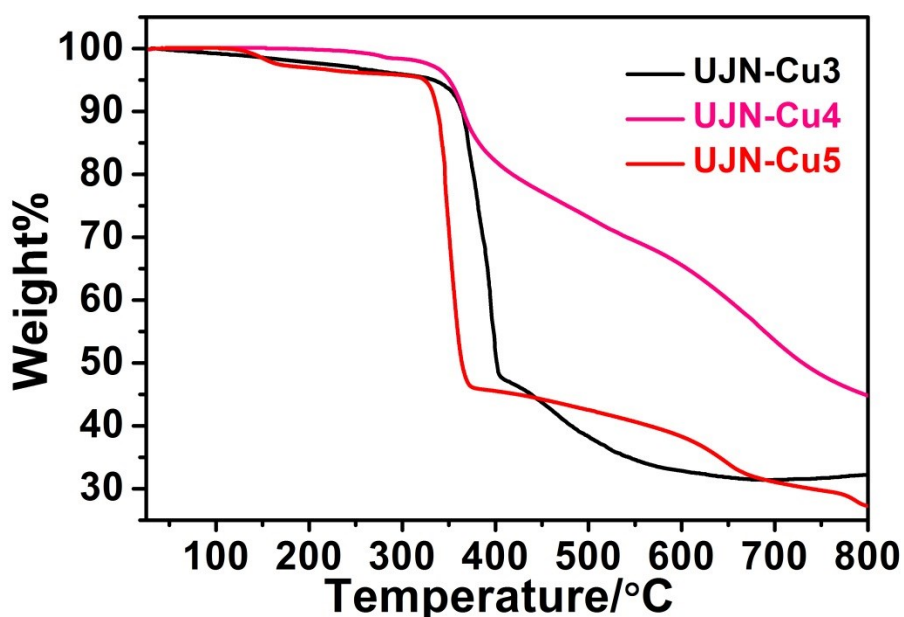


Fig. S3 The TGA curves for UJN-Cu3, UJN-Cu4 and UJN-Cu5, which can remain stable up to 358, 238 and 128 °C.

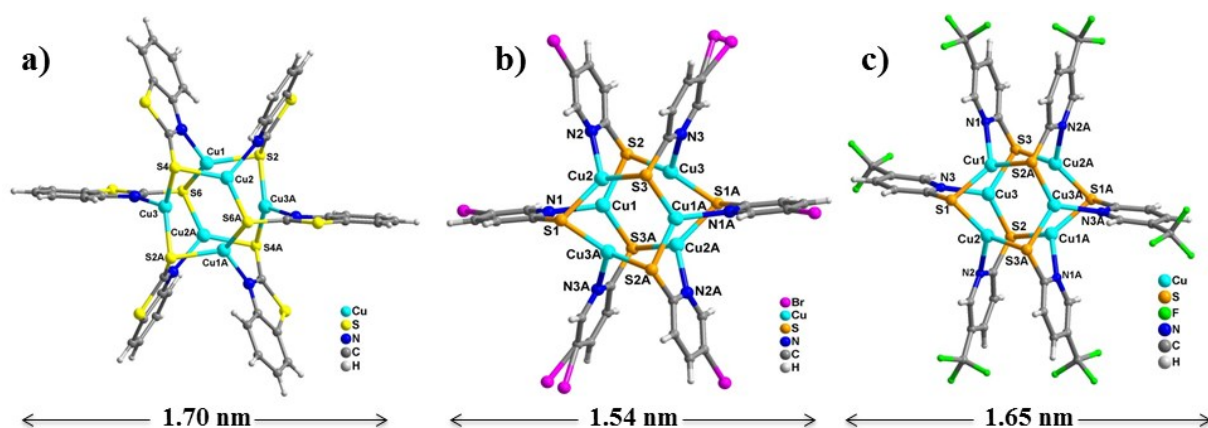


Fig. S4 (a–c) The molecular structures of UJN-Cu3, UJN-Cu4, and UJN-Cu5, respectively. Symmetry codes: A 1-x, 1-y, 1-z.

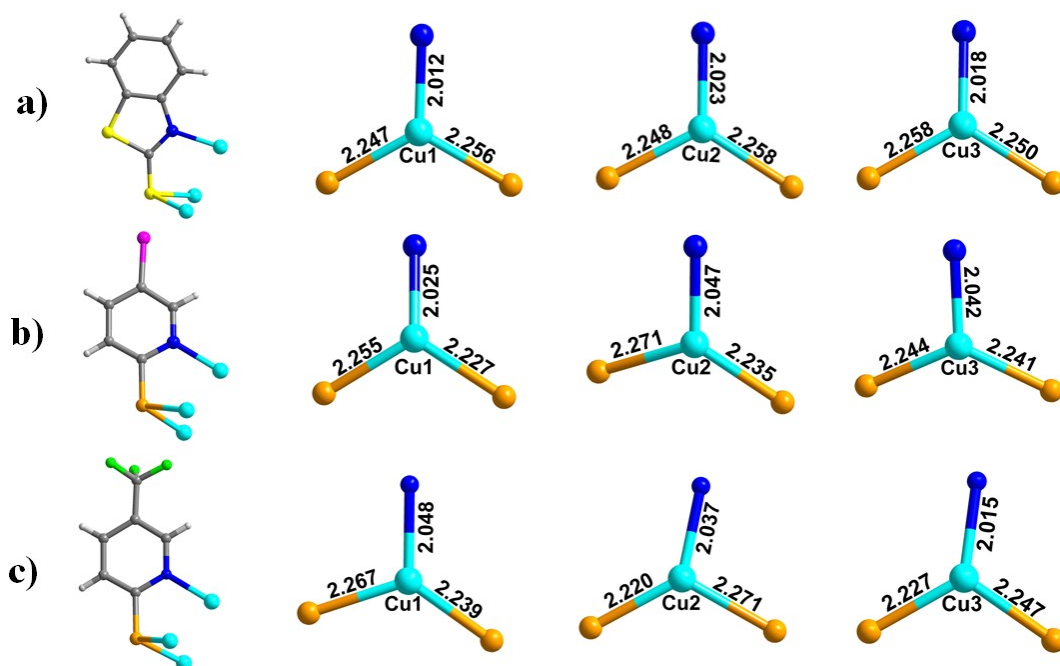


Fig. S5 (a–c) The coordination environments for the N, S donor ligands and copper centers in UJN-Cu3, UJN-Cu4, and UJN-Cu5, respectively.

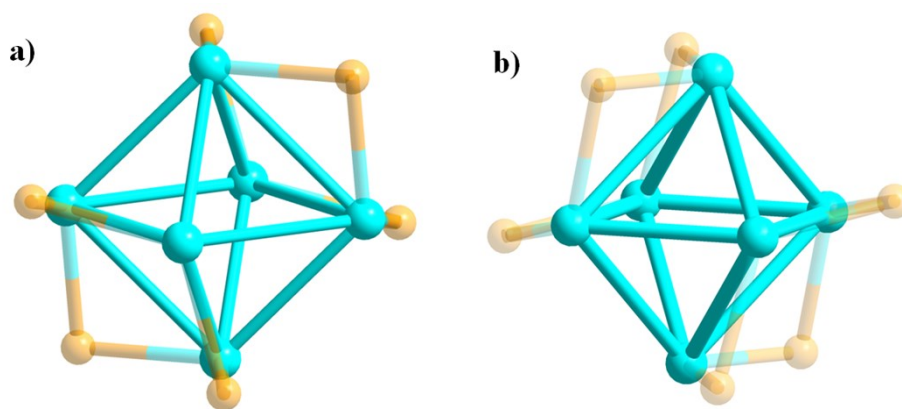


Fig. S6 Octahedral copper(I) core in UJN-Cu3 (a) and UJN-Cu5 (b).

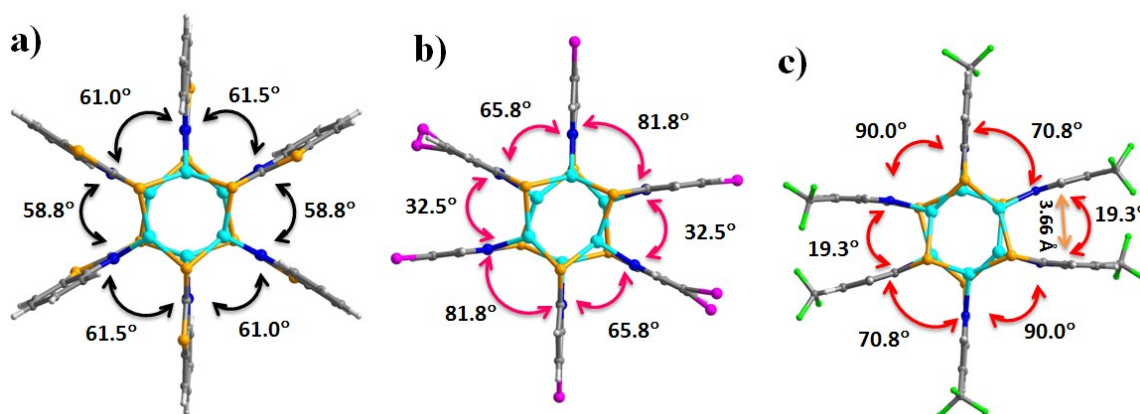


Fig. S7 (a–c) The dihedral angles between neighboring N, S donor ligands, demonstrating the different degree of distortions of UJN-Cu3, UJN-Cu4, and UJN-Cu5, respectively.

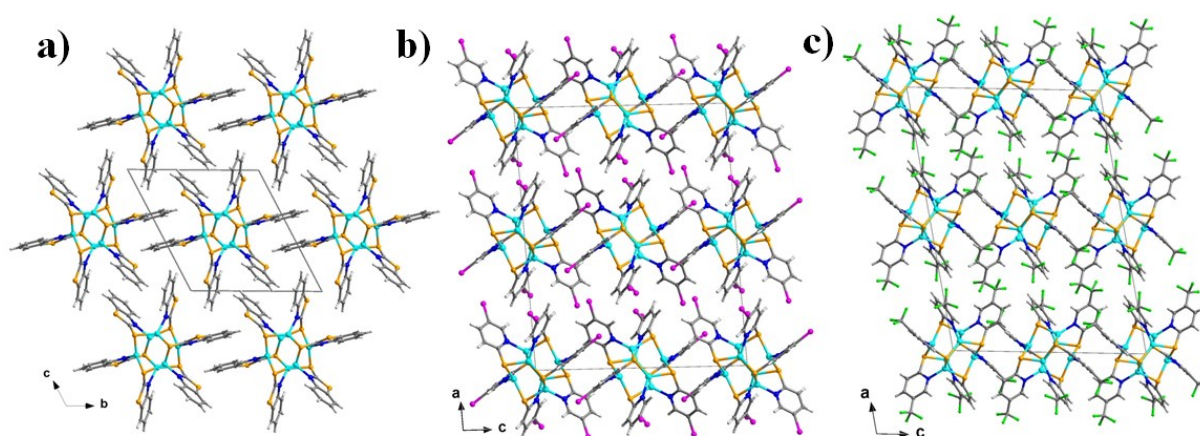


Fig. S8 (a–c) The crystal packing diagrams of UJN-Cu3, UJN-Cu4, and UJN-Cu5, respectively.

Table S3 Distortion analyses of Cu₆ octahedra in UJN-Cu3, UJN-Cu4, and UJN-Cu5.

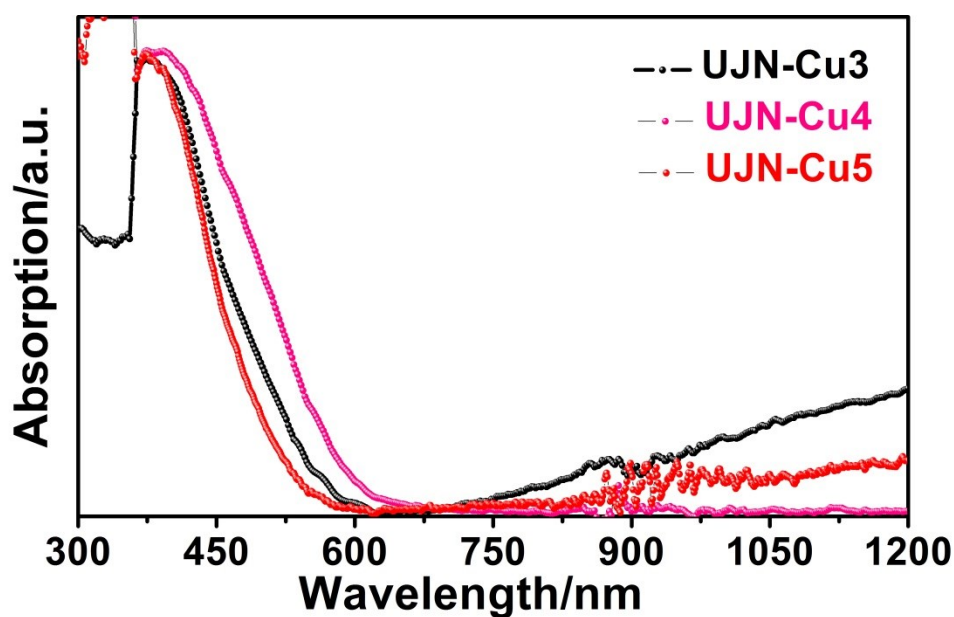
Compound	Cu–Cu length Range	Mean value	Cu–S	Cu–N
UJN-Cu3	2.997–3.097	3.063	2.247–2.258	2.012–2.023
UJN-Cu4	2.767–3.201	2.944	2.227–2.271	2.026–2.047
UJN-Cu5	2.744–3.241	3.002	2.220–2.271	2.015–2.047

Table S4 Dihedral angles between adjacent atomic planes of organic ligands.

Compound	planes 1-2	planes 2-3	planes 3-4	planes 4-5	planes 5-6	planes 6-1
UJN-Cu3	81.8(3)	32.5(3)	65.8(3)	81.8(3)	32.5(3)	65.8(3)
UJN-Cu4	61.5(1)	58.8(2)	61.0(1)	61.5(1)	58.8(2)	61.0(1)
UJN-Cu5	70.8(2)	19.3(2)	90.0(2)	70.8(2)	19.3(2)	90.0(2)

Table S5 Selected hydrogen bonds data for UJN-Cu5.

D–H···A	D–H (Å)	H···A (Å)	D···A (Å)	∠(DHA) (°)
C2–H2···F8	0.93	2.62	3.270	127.5

**Fig. S9** The solid-state UV-Vis absorption spectra for UJN-Cu3, UJN-Cu4, and UJN-Cu5.

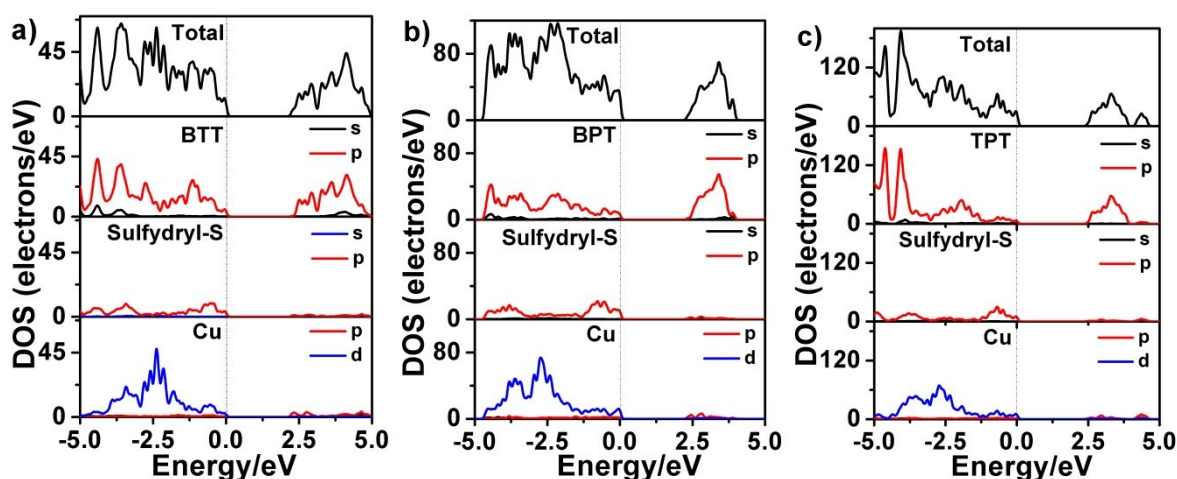


Fig. S10 The partial density of states of (a) UJN-Cu₃, (b) UJN-Cu₄, and (c) UJN-Cu₅.

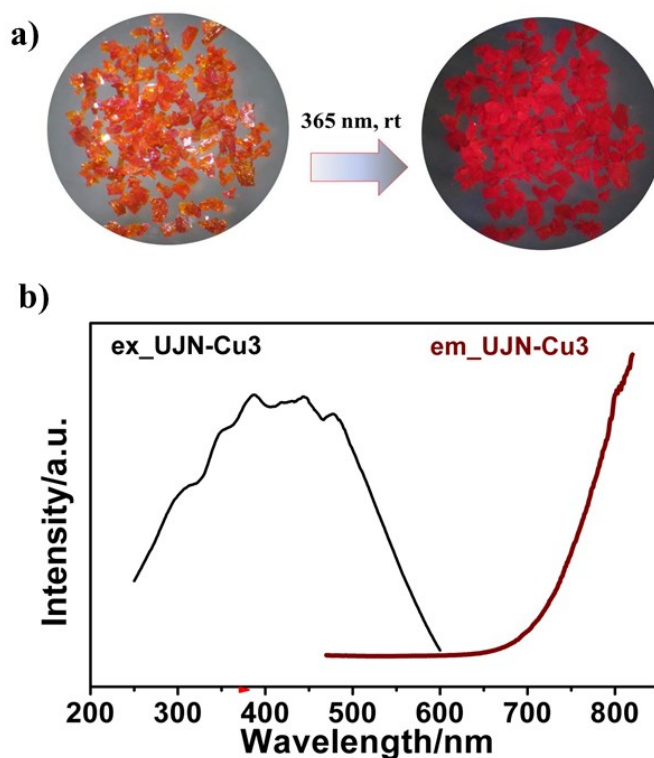


Fig. S11 (a) The optical photos of the single crystals of UJN-Cu₃ under ambient light and 365 nm UV light irradiation. When decreasing the temperature by liquid nitrogen, the dim red light emission of UJN-Cu₃ gradually weakened and vanished finally, which is ascribed to the gradually redshift of the emission band. (b) Solid-state photoluminescence excitation and emission spectra of UJN-Cu₃ at room temperature. The emission spectrum above 800 nm cannot be recorded due to out of the detection range of the machine. Instead, it can be well fitted by the Gauss function with the fitted peak position at 854 nm, and FWHM of 157 nm.

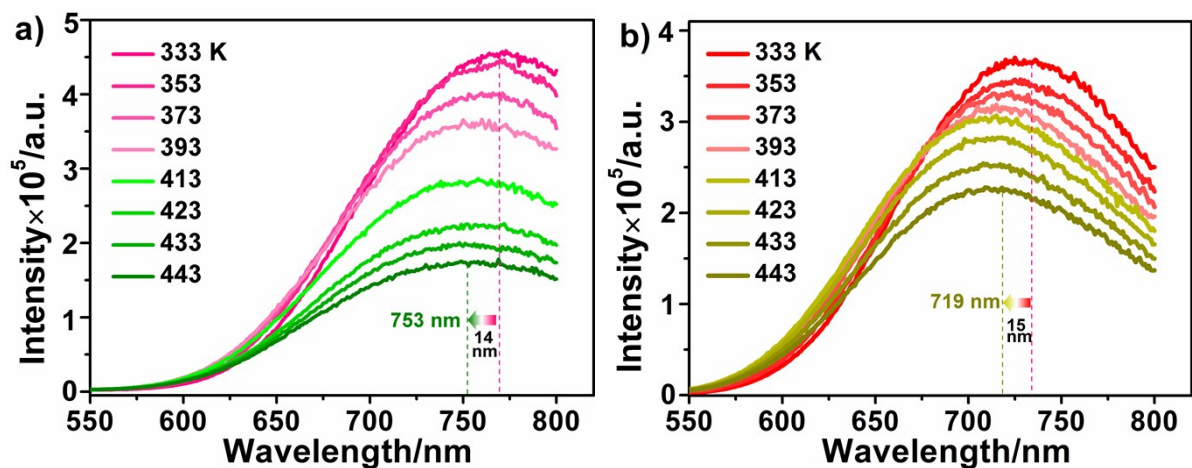


Fig. S12 Temperature dependent solid-state emission spectra for (a) UJN-Cu4 and (b) UJN-Cu5 in the temperature range of 333–443 K. When increasing the temperatures, the emission bands are blueshifted of 14 nm for UJN-Cu4 and 15 nm for UJN-Cu5, accompanied by the weakening of the emission intensity.

Table S6 Important structural and optical data for known hexanuclear copper(I) clusters at room temperature.

Compounds	Shortest Cu–Cu/ Å	λ_{ex} , nm	λ_{em} , nm	Stock shift/nm	QY /%	$\tau/\mu\text{s}$	Reference
UJN-Cu3	3.002	370	792	422	NA	5.54	Reported ¹⁰
	2.997	371	861	490	NA	7.4	Measured
UJN-Cu4	2.767	450	768	287	30%	8.6	This work
UJN-Cu5	2.744	380	738	358	52%	13.1	This work
[Cu ₃ (ptt) ₃] ₂ ·3DMF·3H ₂ O	2.850	390	904	514	4.3	13.9	11
[Cu(ptt) ₆ ·8DMF·7H ₂ O	3.128	360	776	483	1.6	2.88	11
[Cu ₆ (MBID) ₆ (THF) ₆] solution	3.083	300	598	298	NA	8.91	12
[Cu ₃ (mpymt) ₃] ₂	2.865	390	640	250	NA	NA	13
[Cu ₆ (μ_3 -5-phpymt) ₆]	2.776	380	583	203	12.96	NA	14
[Cu ₆ (atdm) ₆]	2.680	290	636	346	NA	NA	15
Y ₂ O ₃ :Eu ³⁺	NA	254	612	358	52%	NA	16

Hptt = 5-(pyridin-4-yl)-1H-1,2,4-triazole-3-thiol, Hmpymt = 4-methyl-pyrimidine-2-thione, 5-phpymt = 5-phenylpyrimidine-2-thiol, atdm = 4-dimethylamino-6-anilino-1,3,5-triazine-2-thiolate

Despite the cuprophilic interaction strength order cannot be handily evaluated by the intermetallic distances, for example, **UJN-Cu4** has a shorter D_{mean} value (mean Cu...Cu distance), but has a slightly longer D_{shortest} value (shortest Cu...Cu distance) than that of **UJN-Cu5**, cuprophilic interactions are still deemed to determine the emission wavelength of **UJN-Cu4** and **UJN-Cu5**. This speculation is supported by the experimental results, where the entangled intermetallic distance between **UJN-Cu4** and **UJN-Cu5** is in accord with their relative close emission maxima, with $\Delta\lambda$ of 30 nm. Meanwhile, the larger deviation of intermetallic distance between **UJN-Cu3** and **UJN-Cu5** generates a longer wave emission for **UJN-Cu3**, with a larger $\Delta\lambda$ value of 123 nm.

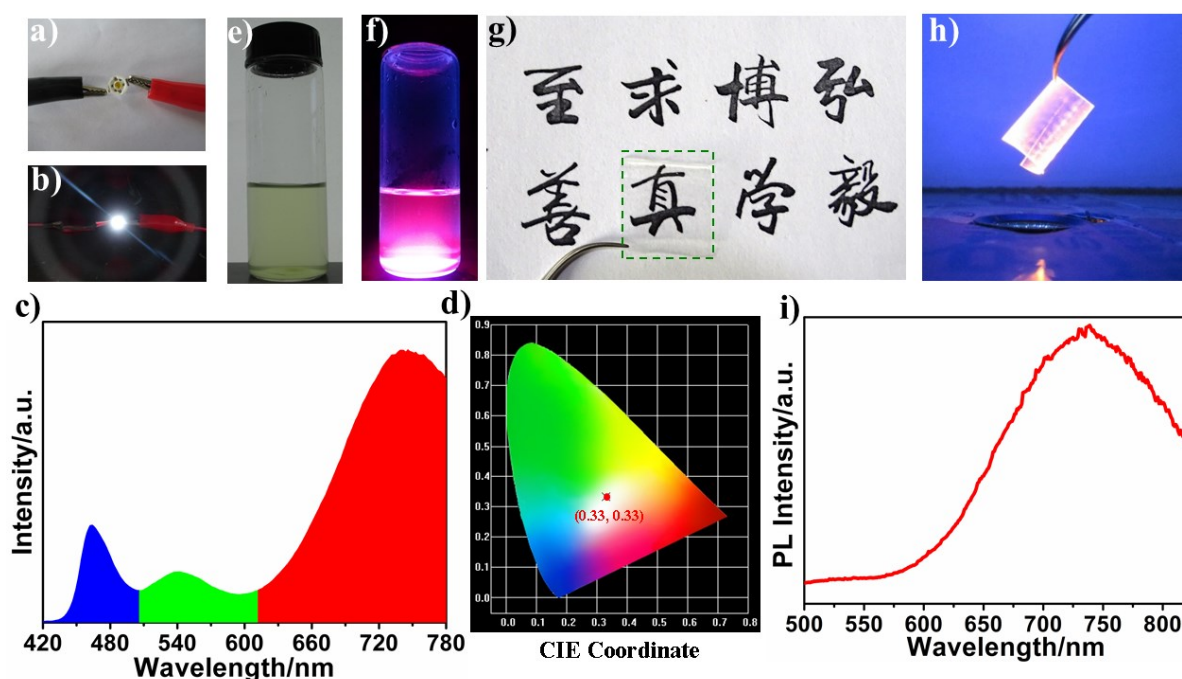


Fig. S13 (a) Showing the fabricated LED chip covered with the modulated white phosphor with **UJN-Cu5**. (b) Lighting the LED chip in panel a. (c) The photoluminescence spectrum of the white LED chip measured by a spectral color illuminometer. (d) The CIE chromaticity coordinates of the modulated white emission. (e-f) The photos of the PMMA solution of **UJN-Cu5** under ambient light and 365 nm UV light irradiation. (g) Demonstration of the

extreme transparency of the PMMA soft film of **UJN-Cu5**. (h) The optical photo of the PMMA soft film under 365 nm UV light irradiation. (i) The emission spectrum of the PMMA soft film of **UJN-Cu5**.

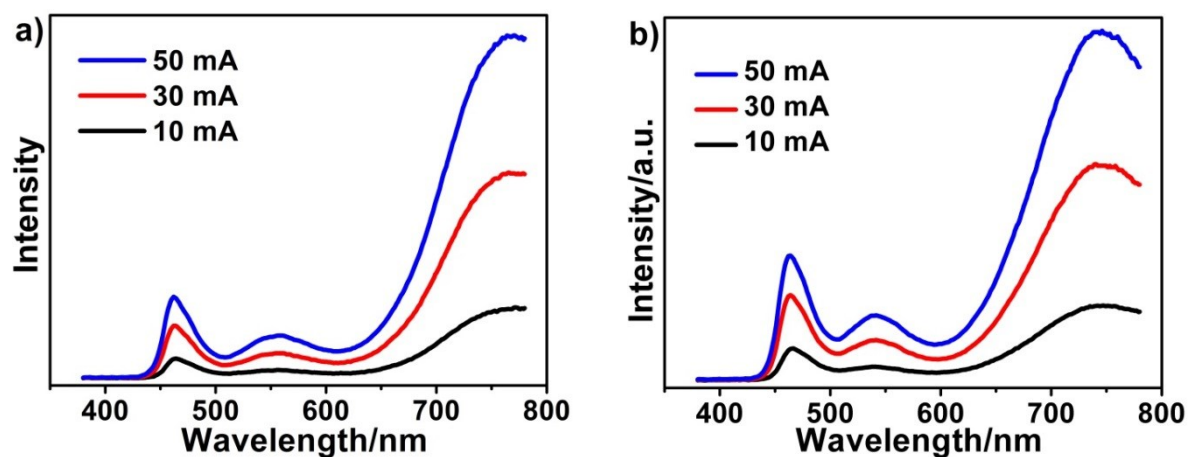


Fig. S14 The solid-state emission spectra of the WLED chips for (a) **UJN-Cu4** and (b) **UJN-Cu5** as a function of current recorded by a spectral color illuminometer.

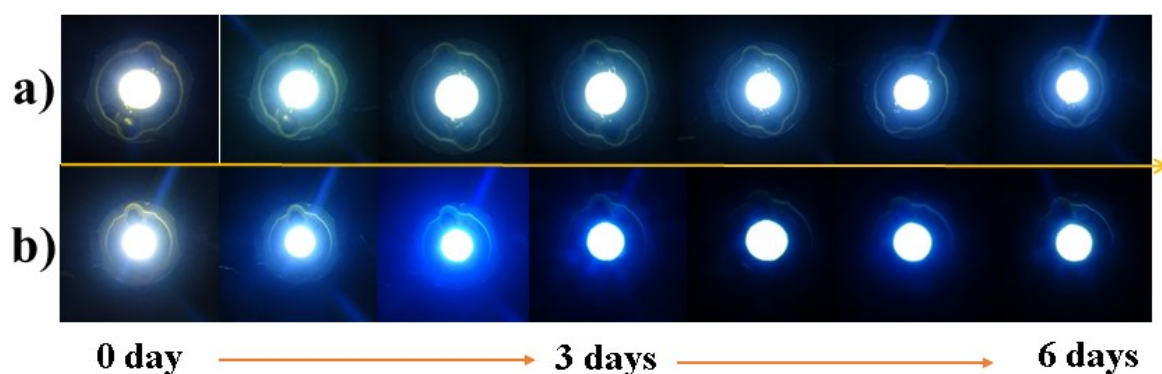


Fig. S15 Photographs of the LED devices fabricated by (a) **UJN-Cu4** and (b) **UJN-Cu5** with continuous lighting for 6 days.

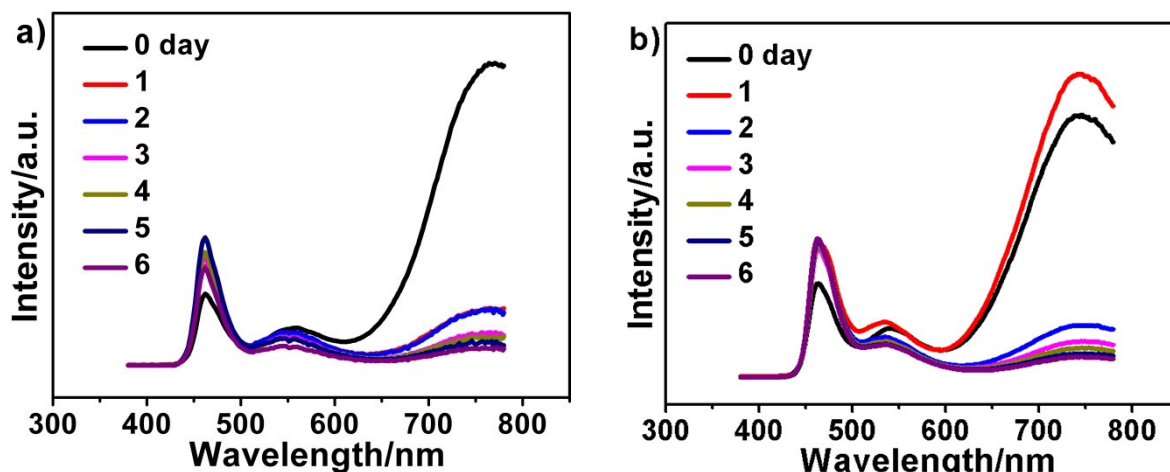


Fig. S16 The emission spectra of the WLED devices fabricated by (a) UJN-Cu4 and (b) UJN-Cu5 with continuous lighting for 6 days.

Table S7 Summary of the LE and CIE coordinate sites of the WLED devices fabricated by UJN-Cu4 and UJN-Cu5 at different days.

Days		0	1	2	3	4	5	6
UJN	LE/%	70	164	166	182	181	185	180
-Cu4	CIE	(0.34,0.34)	(0.26,0.29)	(0.25,0.28)	(0.23,0.26)	(0.23,0.25)	(0.22,0.24)	(0.22,0.23)
UJN	LE/%	83	80	163	175	184	185	189
-Cu5	CIE	(0.33,0.33)	(0.30,0.31)	(0.22,0.28)	(0.22,0.27)	(0.21,0.27)	(0.21,0.25)	(0.20,0.25)

Note: In the endurance test, the devices were set at a constant current of 50 mA and a voltage of 3 V.

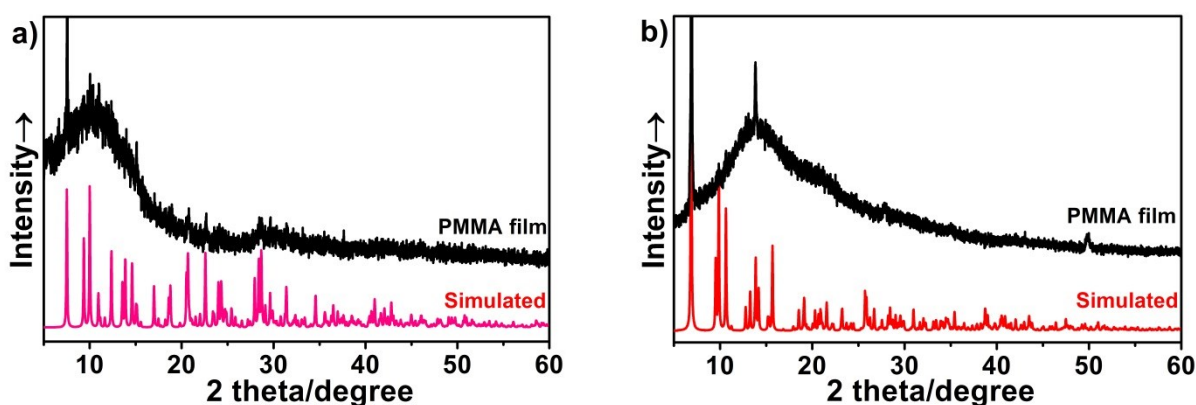
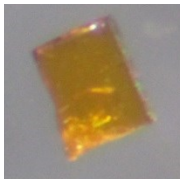
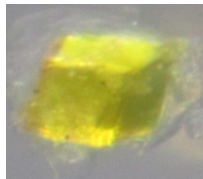


Fig. S17 The powdery diffraction patterns of the fabricated PMMA films (a) UJN-Cu4 and (b) UJN-Cu5 are mainly in accord with their corresponding simulated patterns, which confirms

the stabilities of powdery UJN-Cu4 and Cu5 particles in PMMA films.

Table S8 Photographs and diffraction characterizations of single crystals of UJN-Cu4 and UJN-Cu5 immersed in PMMA acetonitrile solution for 1 day.

Compound	UJN-Cu4-PMMA	UJN-Cu5-PMMA
Morphology		
Diffraction indexing rate/%	94.4	98.4
$a, b, c / \text{\AA}$	23.68(1), 9.54(1), 18.93(1)	26.19(1), 9.58(1), 18.90(1)
$\alpha, \beta, \gamma / ^\circ$	90, 93.4(1), 90	90, 101.0(1), 90
$R_1^a, wR_2^b [I > 2s(I)]$	0.1041, 0.2948	0.0444, 0.1564
$\Delta\rho_{\max}$ and $\Delta\rho_{\min} [e \text{\AA}^{-3}]$	0.79, -0.77	0.71, -0.50

Note: The morphologies of the single crystals remain nearly unchanged after immersed in PMMA acetonitrile solution for 1 day. Further, the PMMA acetonitrile solution-treated single crystals still have good diffraction capabilities and remain cell parameters unchanged.

Table S9 Selected bond distances (\AA) and angles ($^\circ$) for UJN-Cu3, UJN-Cu4 and UJN-Cu5.

UJN-Cu3			
Bond	(\AA)	Bond	(\AA)
Cu(1)-Cu(2)	3.0216(6)	N(1)-C(7)	1.335(4)
Cu(1)-Cu(3)	2.9971(6)	N(2)-C(8)	1.398(4)
Cu(1)-S(2)	2.2564(10)	N(2)-C(14)	1.311(4)
Cu(1)-S(6)	2.2467(9)	N(3)-C(15)	1.392(4)
Cu(1)-N(2)	2.012(3)	N(3)-C(21)	1.311(4)
Cu(2)-S(4)	2.2580(10)	C(1)-C(2)	1.392(6)
Cu(2)-S(6)#1	2.2481(10)	C(1)-C(6)	1.400(6)

Cu(2)-N(1)	2.023(3)	C(2)-C(3)	1.373(6)
Cu(3)-S(2)#1	2.2502(11)	C(3)-C(4)	1.365(8)
Cu(3)-S(4)	2.2577(10)	C(4)-C(5)	1.355(8)
Cu(3)-N(3)	2.019(3)	C(5)-C(6)	1.398(6)
S(1)-C(6)	1.737(5)	C(8)-C(9)	1.397(5)
S(1)-C(7)	1.847(4)	C(8)-C(13)	1.387(5)
S(2)-Cu(3)#1	2.2502(11)	C(9)-C(10)	1.381(6)
S(2)-C(7)	1.611(4)	C(10)-C(11)	1.367(6)
S(3)-C(13)	1.743(4)	C(11)-C(12)	1.376(6)
S(3)-C(14)	1.748(4)	C(12)-C(13)	1.386(5)
S(4)-C(14)	1.726(4)	C(15)-C(16)	1.399(5)
S(5)-C(20)	1.735(4)	C(15)-C(20)	1.392(5)
S(5)-C(21)	1.742(3)	C(16)-C(17)	1.379(6)
S(6)-Cu(2)#1	2.2482(10)	C(17)-C(18)	1.377(7)
S(6)-C(21)	1.732(3)	C(18)-C(19)	1.357(7)
N(1)-C(1)	1.389(4)	C(19)-C(20)	1.388(6)
Angle	(°)	Angle	(°)
Cu(3)-Cu(1)-Cu(2)	61.926(16)	C(21)-N(3)-Cu(3)	122.7(2)
S(2)-Cu(1)-Cu(2)	79.60(3)	C(21)-N(3)-C(15)	111.6(3)
S(2)-Cu(1)-Cu(3)	134.53(3)	N(1)-C(1)-C(2)	126.3(4)
S(6)-Cu(1)-Cu(2)	135.09(3)	N(1)-C(1)-C(6)	114.5(3)
S(6)-Cu(1)-Cu(3)	80.24(3)	C(2)-C(1)-C(6)	119.2(4)
S(6)-Cu(1)-S(2)	117.54(4)	C(3)-C(2)-C(1)	118.5(4)
N(2)-Cu(1)-Cu(2)	80.05(8)	C(4)-C(3)-C(2)	121.9(5)
N(2)-Cu(1)-Cu(3)	81.05(8)	C(5)-C(4)-C(3)	121.2(5)
N(2)-Cu(1)-S(2)	116.89(8)	C(4)-C(5)-C(6)	118.4(5)
N(2)-Cu(1)-S(6)	118.90(8)	C(1)-C(6)-S(1)	109.0(3)
S(4)-Cu(2)-Cu(1)	79.85(3)	C(5)-C(6)-S(1)	130.2(4)

S(6)#1-Cu(2)-Cu(1)	131.89(3)	C(5)-C(6)-C(1)	120.8(4)
S(6)#1-Cu(2)-S(4)	117.89(4)	S(2)-C(7)-S(1)	119.99(19)
N(1)-Cu(2)-Cu(1)	82.28(8)	N(1)-C(7)-S(1)	106.6(3)
N(1)-Cu(2)-S(4)	120.41(9)	N(1)-C(7)-S(2)	133.4(3)
N(1)-Cu(2)-S(6)#1	116.26(9)	C(9)-C(8)-N(2)	124.6(3)
S(2)#1-Cu(3)-Cu(1)	132.27(3)	C(13)-C(8)-N(2)	115.1(3)
S(2)#1-Cu(3)-S(4)	117.83(4)	C(13)-C(8)-C(9)	120.3(3)
S(4)-Cu(3)-Cu(1)	80.41(3)	C(10)-C(9)-C(8)	117.6(4)
N(3)-Cu(3)-Cu(1)	80.72(8)	C(11)-C(10)-C(9)	121.6(4)
N(3)-Cu(3)-S(2)#1	118.77(8)	C(10)-C(11)-C(12)	121.6(4)
N(3)-Cu(3)-S(4)	117.56(9)	C(11)-C(12)-C(13)	117.7(4)
C(6)-S(1)-C(7)	92.37(18)	C(8)-C(13)-S(3)	109.1(3)
Cu(3)#1-S(2)-Cu(1)	86.64(4)	C(12)-C(13)-S(3)	129.7(3)
C(7)-S(2)-Cu(1)	100.33(12)	C(12)-C(13)-C(8)	121.2(3)
C(7)-S(2)-Cu(3)#1	101.45(12)	S(4)-C(14)-S(3)	120.77(18)
C(13)-S(3)-C(14)	90.07(17)	N(2)-C(14)-S(3)	114.1(3)
Cu(3)-S(4)-Cu(2)	86.59(4)	N(2)-C(14)-S(4)	125.2(3)
C(14)-S(4)-Cu(2)	101.59(11)	N(3)-C(15)-C(16)	125.3(3)
C(14)-S(4)-Cu(3)	100.10(11)	N(3)-C(15)-C(20)	114.9(3)
C(20)-S(5)-C(21)	90.07(17)	C(20)-C(15)-C(16)	119.8(3)
Cu(1)-S(6)-Cu(2)#1	86.84(3)	C(17)-C(16)-C(15)	117.9(4)
C(21)-S(6)-Cu(1)	102.88(11)	C(18)-C(17)-C(16)	121.5(4)
C(21)-S(6)-Cu(2)#1	101.02(12)	C(19)-C(18)-C(17)	121.2(4)
C(1)-N(1)-Cu(2)	125.0(2)	C(18)-C(19)-C(20)	118.6(4)
C(7)-N(1)-Cu(2)	117.2(2)	C(15)-C(20)-S(5)	109.2(3)
C(7)-N(1)-C(1)	117.5(3)	C(19)-C(20)-S(5)	129.9(3)
C(8)-N(2)-Cu(1)	124.3(2)	C(19)-C(20)-C(15)	120.9(4)
C(14)-N(2)-Cu(1)	123.8(2)	S(6)-C(21)-S(5)	120.34(19)
C(14)-N(2)-C(8)	111.7(3)	N(3)-C(21)-S(5)	114.3(3)

C(15)-N(3)-Cu(3)	125.2(2)	N(3)-C(21)-S(6)	125.3(2)
------------------	----------	-----------------	----------

Symmetry transformations used to generate equivalent atoms: #1 -x+1,-y+1,-z+1.

UJN-Cu4			
Bond	(Å)	Bond	(Å)
Br(1)-C(2)	1.881(11)	S(1)-C(5)	1.750(10)
Br(2)-C(7)	1.916(9)	S(2)-C(10)	1.742(8)
Br(3)-Br(3B)	0.749(18)	S(3)-Cu(1)#1	2.255(2)
Br(3)-C(12)	1.908(12)	S(3)-C(15)	1.751(10)
Br(3B)-C(12)	1.950(15)	N(1)-C(1)	1.325(12)
Cu(1)-Cu(2)	2.7699(17)	N(1)-C(5)	1.342(10)
Cu(1)-Cu(3)	3.0340(18)	N(2)-C(6)	1.341(10)
Cu(1)-Cu(3)#1	2.7672(15)	N(2)-C(10)	1.343(10)
Cu(1)-S(2)	2.227(2)	N(3)-C(11)	1.335(11)
Cu(1)-S(3)#1	2.255(2)	N(3)-C(15)	1.343(10)
Cu(1)-N(1)	2.026(7)	C(1)-C(2)	1.388(14)
Cu(2)-Cu(3)	2.9597(14)	C(2)-C(3)	1.373(14)
Cu(2)-Cu(3)#1	2.9375(15)	C(3)-C(4)	1.368(14)
Cu(2)-S(1)	2.235(3)	C(4)-C(5)	1.389(11)
Cu(2)-S(3)	2.271(3)	C(6)-C(7)	1.369(12)
Cu(2)-N(2)	2.047(6)	C(7)-C(8)	1.366(13)
Cu(3)-Cu(1)#1	2.7672(15)	C(8)-C(9)	1.345(13)
Cu(3)-Cu(2)#1	2.9375(15)	C(9)-C(10)	1.389(11)
Cu(3)-S(1)#1	2.241(2)	C(11)-C(12)	1.338(14)
Cu(3)-S(2)	2.244(3)	C(12)-C(13)	1.371(14)
Cu(3)-N(3)	2.043(8)	C(13)-C(14)	1.374(14)
S(1)-Cu(3)#1	2.241(2)	C(14)-C(15)	1.395(13)
Angle	(°)	Angle	(°)

Br(3B)-Br(3)-C(12)	82.0(13)	N(3)-Cu(3)-S(1)#1	116.8(2)
Br(3)-Br(3B)-C(12)	75.7(14)	N(3)-Cu(3)-S(2)	108.8(2)
Cu(2)-Cu(1)-Cu(3)	61.12(4)	Cu(2)-S(1)-Cu(3)#1	82.04(8)
Cu(3)#1-Cu(1)-Cu(2)	64.08(4)	C(5)-S(1)-Cu(2)	108.1(3)
Cu(3)#1-Cu(1)-Cu(3)	88.19(5)	C(5)-S(1)-Cu(3)#1	104.6(3)
S(2)-Cu(1)-Cu(2)	77.98(7)	Cu(1)-S(2)-Cu(3)	85.46(8)
S(2)-Cu(1)-Cu(3)#1	132.72(9)	C(10)-S(2)-Cu(1)	112.0(3)
S(2)-Cu(1)-Cu(3)	47.50(7)	C(10)-S(2)-Cu(3)	102.2(3)
S(2)-Cu(1)-S(3)#1	115.37(8)	Cu(1)#1-S(3)-Cu(2)	90.04(10)
S(3)#1-Cu(1)-Cu(2)	134.36(9)	C(15)-S(3)-Cu(1)#1	107.4(3)
S(3)#1-Cu(1)-Cu(3)#1	78.06(7)	C(15)-S(3)-Cu(2)	102.6(3)
S(3)#1-Cu(1)-Cu(3)	94.78(8)	C(1)-N(1)-Cu(1)	121.8(6)
N(1)-Cu(1)-Cu(2)	89.4(2)	C(1)-N(1)-C(5)	118.6(8)
N(1)-Cu(1)-Cu(3)#1	86.6(2)	C(5)-N(1)-Cu(1)	119.6(7)
N(1)-Cu(1)-Cu(3)	149.1(2)	C(6)-N(2)-Cu(2)	121.6(6)
N(1)-Cu(1)-S(2)	121.5(2)	C(6)-N(2)-C(10)	120.3(7)
N(1)-Cu(1)-S(3)#1	113.8(2)	C(10)-N(2)-Cu(2)	117.3(5)
Cu(1)-Cu(2)-Cu(3)	63.85(4)	C(11)-N(3)-Cu(3)	121.2(6)
Cu(1)-Cu(2)-Cu(3)#1	57.92(4)	C(11)-N(3)-C(15)	119.6(8)
Cu(3)#1-Cu(2)-Cu(3)	86.52(4)	C(15)-N(3)-Cu(3)	119.1(6)
S(1)-Cu(2)-Cu(1)	77.96(7)	N(1)-C(1)-C(2)	123.2(9)
S(1)-Cu(2)-Cu(3)#1	49.07(6)	C(1)-C(2)-Br(1)	119.9(8)
S(1)-Cu(2)-Cu(3)	133.15(7)	C(3)-C(2)-Br(1)	122.2(9)
S(1)-Cu(2)-S(3)	119.40(9)	C(3)-C(2)-C(1)	118.0(11)
S(3)-Cu(2)-Cu(1)	130.72(7)	C(4)-C(3)-C(2)	119.5(9)
S(3)-Cu(2)-Cu(3)	73.77(6)	C(3)-C(4)-C(5)	119.5(9)
S(3)-Cu(2)-Cu(3)#1	97.08(7)	N(1)-C(5)-S(1)	118.2(7)
N(2)-Cu(2)-Cu(1)	91.2(2)	N(1)-C(5)-C(4)	121.3(9)
N(2)-Cu(2)-Cu(3)	84.32(18)	C(4)-C(5)-S(1)	120.5(7)

N(2)-Cu(2)-Cu(3)#1	148.6(2)	N(2)-C(6)-C(7)	120.7(8)
N(2)-Cu(2)-S(1)	124.2(2)	C(6)-C(7)-Br(2)	118.8(7)
N(2)-Cu(2)-S(3)	109.0(2)	C(8)-C(7)-Br(2)	120.9(7)
Cu(1)#1-Cu(3)-Cu(1)	91.81(5)	C(8)-C(7)-C(6)	120.3(8)
Cu(1)#1-Cu(3)-Cu(2)	67.87(4)	C(9)-C(8)-C(7)	118.1(8)
Cu(1)#1-Cu(3)-Cu(2)#1	58.00(4)	C(8)-C(9)-C(10)	121.7(8)
Cu(2)-Cu(3)-Cu(1)	55.03(4)	N(2)-C(10)-S(2)	119.9(6)
Cu(2)#1-Cu(3)-Cu(1)	64.81(4)	N(2)-C(10)-C(9)	118.9(7)
Cu(2)#1-Cu(3)-Cu(2)	93.48(4)	C(9)-C(10)-S(2)	121.1(6)
S(1)#1-Cu(3)-Cu(1)	107.30(8)	N(3)-C(11)-C(12)	122.4(9)
S(1)#1-Cu(3)-Cu(1)#1	77.92(6)	Br(3)-C(12)-Br(3B)	22.3(5)
S(1)#1-Cu(3)-Cu(2)	139.61(7)	C(11)-C(12)-Br(3)	120.4(8)
S(1)#1-Cu(3)-Cu(2)#1	48.89(6)	C(11)-C(12)-Br(3B)	116.2(9)
S(1)#1-Cu(3)-S(2)	123.78(10)	C(11)-C(12)-C(13)	120.0(10)
S(2)-Cu(3)-Cu(1)	47.03(6)	C(13)-C(12)-Br(3)	118.5(9)
S(2)-Cu(3)-Cu(1)#1	135.72(8)	C(13)-C(12)-Br(3B)	122.4(9)
S(2)-Cu(3)-Cu(2)	73.68(6)	C(12)-C(13)-C(14)	118.5(11)
S(2)-Cu(3)-Cu(2)#1	104.69(8)	C(13)-C(14)-C(15)	119.6(10)
N(3)-Cu(3)-Cu(1)#1	88.41(19)	N(3)-C(15)-S(3)	118.7(7)
N(3)-Cu(3)-Cu(1)	134.86(19)	N(3)-C(15)-C(14)	119.9(8)
N(3)-Cu(3)-Cu(2)	83.87(19)	C(14)-C(15)-S(3)	121.4(7)
N(3)-Cu(3)-Cu(2)#1	144.1(2)		

Symmetry transformations used to generate equivalent atoms: #1 -x+1,-y+1,-z+1.

UJN-Cu5			
Bond	(Å)	Bond	(Å)
Cu(1)-Cu(2)	2.9976(12)	F(8)-C(11)	1.313(12)
Cu(1)-Cu(3)	2.7473(12)	F(9)-C(11)	1.310(11)
Cu(1)-S(1)	2.2394(18)	N(1)-C(1)	1.354(9)

Cu(1)-S(2)#1	2.2669(19)	N(1)-C(5)	1.338(9)
Cu(1)-N(1)	2.047(6)	N(2)-C(13)	1.340(8)
Cu(2)-Cu(3)	2.7435(12)	N(2)-C(17)	1.351(9)
Cu(2)-S(1)	2.2197(19)	N(3)-C(7)	1.339(9)
Cu(2)-S(3)#1	2.271(2)	N(3)-C(12)	1.348(9)
Cu(2)-N(2)	2.037(5)	C(1)-C(2)	1.377(10)
Cu(3)-S(2)	2.2271(19)	C(2)-C(3)	1.374(11)
Cu(3)-S(3)	2.2466(18)	C(3)-C(4)	1.384(11)
Cu(3)-N(3)	2.015(6)	C(4)-C(5)	1.371(11)
S(1)-C(7)	1.762(7)	C(4)-C(6)	1.478(11)
S(2)-Cu(1)#1	2.2667(19)	C(7)-C(8)	1.405(9)
S(2)-C(13)	1.758(6)	C(8)-C(9)	1.372(11)
S(3)-Cu(2)#1	2.271(2)	C(9)-C(10)	1.379(11)
S(3)-C(1)	1.758(7)	C(10)-C(11)	1.477(12)
F(1)-C(6)	1.342(12)	C(10)-C(12)	1.385(11)
F(2)-C(6)	1.272(12)	C(13)-C(14)	1.386(9)
F(3)-C(6)	1.324(12)	C(14)-C(15)	1.361(11)
F(4)-C(18)	1.319(10)	C(15)-C(16)	1.393(10)
F(5)-C(18)	1.306(10)	C(16)-C(17)	1.371(10)
F(6)-C(18)	1.283(11)	C(16)-C(18)	1.472(10)
F(7)-C(11)	1.312(12)		
Angle	(°)	Angle	(°)
Cu(3)-Cu(1)-Cu(2)	56.85(3)	C(12)-N(3)-Cu(3)	122.5(5)
S(1)-Cu(1)-Cu(2)	47.48(5)	N(1)-C(1)-S(3)	119.1(5)
S(1)-Cu(1)-Cu(3)	77.02(5)	N(1)-C(1)-C(2)	120.8(6)
S(1)-Cu(1)-S(2)#1	122.32(7)	C(2)-C(1)-S(3)	120.0(5)
S(2)#1-Cu(1)-Cu(2)	100.32(5)	C(3)-C(2)-C(1)	120.1(7)
S(2)#1-Cu(1)-Cu(3)	130.18(6)	C(2)-C(3)-C(4)	118.9(7)

N(1)-Cu(1)-Cu(2)	146.66(16)	C(3)-C(4)-C(6)	120.5(8)
N(1)-Cu(1)-Cu(3)	90.84(16)	C(5)-C(4)-C(3)	118.5(7)
N(1)-Cu(1)-S(1)	123.18(17)	C(5)-C(4)-C(6)	120.9(8)
N(1)-Cu(1)-S(2)#1	107.89(17)	N(1)-C(5)-C(4)	122.9(7)
Cu(3)-Cu(2)-Cu(1)	56.97(3)	F(1)-C(6)-C(4)	111.9(8)
S(1)-Cu(2)-Cu(1)	48.04(5)	F(2)-C(6)-F(1)	108.8(10)
S(1)-Cu(2)-Cu(3)	77.41(5)	F(2)-C(6)-F(3)	105.3(9)
S(1)-Cu(2)-S(3)#1	120.41(7)	F(2)-C(6)-C(4)	113.4(9)
S(3)#1-Cu(2)-Cu(1)	98.16(5)	F(3)-C(6)-F(1)	102.0(9)
S(3)#1-Cu(2)-Cu(3)	129.61(6)	F(3)-C(6)-C(4)	114.8(8)
N(2)-Cu(2)-Cu(1)	149.49(16)	N(3)-C(7)-S(1)	117.6(5)
N(2)-Cu(2)-Cu(3)	92.96(15)	N(3)-C(7)-C(8)	120.8(6)
N(2)-Cu(2)-S(1)	126.41(16)	C(8)-C(7)-S(1)	121.5(5)
N(2)-Cu(2)-S(3)#1	106.31(17)	C(9)-C(8)-C(7)	119.8(7)
Cu(2)-Cu(3)-Cu(1)	66.18(3)	C(8)-C(9)-C(10)	119.3(7)
S(2)-Cu(3)-Cu(1)	133.83(6)	C(9)-C(10)-C(11)	121.8(8)
S(2)-Cu(3)-Cu(2)	77.35(5)	C(9)-C(10)-C(12)	118.4(7)
S(2)-Cu(3)-S(3)	112.81(7)	C(12)-C(10)-C(11)	119.8(8)
S(3)-Cu(3)-Cu(1)	78.04(5)	F(7)-C(11)-F(8)	103.8(9)
S(3)-Cu(3)-Cu(2)	134.44(6)	F(7)-C(11)-C(10)	113.8(9)
N(3)-Cu(3)-Cu(1)	85.70(17)	F(8)-C(11)-C(10)	114.0(8)
N(3)-Cu(3)-Cu(2)	91.27(17)	F(9)-C(11)-F(7)	105.6(8)
N(3)-Cu(3)-S(2)	123.61(17)	F(9)-C(11)-F(8)	102.9(10)
N(3)-Cu(3)-S(3)	113.91(18)	F(9)-C(11)-C(10)	115.3(8)
Cu(2)-S(1)-Cu(1)	84.48(7)	N(3)-C(12)-C(10)	122.7(7)
C(7)-S(1)-Cu(1)	103.4(2)	N(2)-C(13)-S(2)	118.7(5)
C(7)-S(1)-Cu(2)	108.3(2)	N(2)-C(13)-C(14)	121.2(6)
Cu(3)-S(2)-Cu(1)#1	90.78(7)	C(14)-C(13)-S(2)	120.0(5)
C(13)-S(2)-Cu(1)#1	100.1(2)	C(15)-C(14)-C(13)	119.9(6)

C(13)-S(2)-Cu(3)	113.4(2)	C(14)-C(15)-C(16)	119.4(7)
Cu(3)-S(3)-Cu(2)#1	91.69(7)	C(15)-C(16)-C(18)	121.3(7)
C(1)-S(3)-Cu(2)#1	102.3(2)	C(17)-C(16)-C(15)	117.8(7)
C(1)-S(3)-Cu(3)	109.7(2)	C(17)-C(16)-C(18)	120.7(6)
C(1)-N(1)-Cu(1)	117.5(5)	N(2)-C(17)-C(16)	123.0(6)
C(5)-N(1)-Cu(1)	123.3(5)	F(4)-C(18)-C(16)	113.9(7)
C(5)-N(1)-C(1)	118.7(6)	F(5)-C(18)-F(4)	101.6(7)
C(13)-N(2)-Cu(2)	117.1(4)	F(5)-C(18)-C(16)	114.3(7)
C(13)-N(2)-C(17)	118.4(6)	F(6)-C(18)-F(4)	105.1(8)
C(17)-N(2)-Cu(2)	122.6(4)	F(6)-C(18)-F(5)	108.7(8)
C(7)-N(3)-Cu(3)	118.5(5)	F(6)-C(18)-C(16)	112.3(7)
C(7)-N(3)-C(12)	119.0(6)		

Symmetry transformations used to generate equivalent atoms: #1 -x+1,-y+1,-z+1.

Reference

1. W. M. Wendlandt and H. G. Hecht, *Reflectance Spectroscopy*. Interscience: New York, 1966.
2. K. Wu, A. Bera, C. Ma, Y. Du, Y. Yang, L. Li and T. Wu, *Phys. Chem. Chem. Phys.*, 2014, **16**, 22476-22481.
3. M. D. Segall, P. J. D. Lindan, M. J. Probert, C. J. Pickard, P. J. Hasnip, S. J. Clark and M. C. Payne, *J. Phys.: Condens. Matter*, 2002, **14**, 2717-2744.
4. V. Milman, B. Winkler, J. A. White, C. J. Pickard, M. C. Payne, E. V. Akhmatkaya and R. H. Nobes, *Int. J. Quantum Chem.*, 2000, **77**, 895-910.
5. D. R. Hamann, M. Schluter and C. Chiang, *Phys. Rev. Lett.*, 1979, **43**, 1494-1497.
6. M.J. Frisch, G.W. Trucks, H.B. Schlegel, G. E. Scuseria, M. A. Robb, J. R. Cheeseman, et al. (2013) Gaussian 09, Revision D.01. Gaussian Inc., Wallingford CT.
7. Agilent, *CrysAlisPro*. Version 1.171.35.21 ed.; Agilent Technologies Corp.: California, America.
8. Siemens, *SHELXTL Version 5 Reference manual*. Siemens Energy & Automation Inc.:

Madison, WI, 1994.

9. M. J. Turner, J. J. McKinnon, S. K. Wolff, D. J. Grimwood, P. R. Spackman, D. Jayatilaka and M. A. Spackman CrystalExplorer17. <https://hirshfeldsurface.net>.
10. S. Sun, L.-J. Liu, W.-Y. Ma, W.-X. Zhou, J. Li and F.-X. Zhang, *J. Solid State Chem.*, 2015, **225**, 1-7.
11. X.-C. Shan, F.-L. Jiang, D.-Q. Yuan, M.-Y. Wu, S.-Q. Zhang and M.-C. Hong, *Dalton Trans.*, 2012, **41**, 9411-9416.
12. A. Singh, A. Singh, N. Singh and D. O. Jang, *Sens. Actuators, B-Chem.*, 2017, **243**, 372-379.
13. J. F. Song, S. Z. Li, R. S. Zhou, J. Shao, X. M. Qiu, Y. Y. Jia, J. Wang and X. Zhang, *Dalton Trans.*, 2016, **45**, 11883-11891.
14. M.-J. Zhang, H.-X. Li, H.-Y. Li and J.-P. Lang, *Dalton Trans.*, 2016, **45**, 17759-17769.
15. S. Hu, F.-Y. Yu, P. Zhang and D.-R. Lin, *Dalton Trans.*, 2013, **42**, 7731-7740.
16. W.-N. Wang, W. Widiyastuti, T. Ogi, I. W. Lenggoro, and K. Okuyama, *Chem. Mater.*, 2007, **19**, 1723-1730.